Neoplasma 2023; 70(2): 240–250

doi:10.4149/neo_2023_221209N1173

Transcriptional adaptor 3 influences the proliferative and invasive phenotypes of non-small cell lung cancer cells via regulating EMT

Li-Qin XU[1,2], Shu-Wen ZHANG[2], Rui ZHANG[2], Jing-Jing CHEN[2], Zai-Xin YUAN[2], Jian FENG[2], Jian-An HUANG[1,*]

[1]Department of Pulmonary and Critical Care Medicine, The First Affiliated Hospital of Soochow University, Suzhou, Jiangsu, China; [2]Department of Pulmonary and Critical Care Medicine, Affiliated Hospital of Nantong University, Nantong, Jiangsu, China

**Correspondence: huang_jian_an@163.com*

Received December 9, 2022 / Accepted March 16, 2023

Transcriptional adaptor 3 (TADA3/ADA3) is a conserved transcriptional co-activator and is dysregulated in many aggressive tumors. However, the role of TADA3 in non-small cell lung cancer (NSCLC) remains unknown. It was previously demonstrated that TADA3 expression correlates with poor prognosis in patients with NSCLC. In the present study, the expression and function of TADA3 were investigated in cells *in vitro* and *in vivo*. TADA3 expression was evaluated in clinical specimens and cell lines using reverse transcription-quantitative PCR and western blot analysis. The TADA3 protein level was significantly higher in human NSCLC specimens compared with matched normal tissues. In human NSCLC cell lines, short hairpin RNA-mediated silencing of TADA3 suppressed their proliferative, migratory and invasive abilities *in vitro*, and delayed G1 to S phase progression through the cell cycle. Consistent with this, TADA3 silencing increased expression of the epithelial marker E-cadherin and reduced expression of the mesenchymal markers, N-cadherin, Vimentin, Snail, and Slug. To verify the effect of TADA3 on tumor formation and growth *in vivo*, a mouse tumor xenograft model was established. TADA3 silencing slowed the growth of NSCLC tumor xenografts in nude mice, and excised tumors showed a similarly altered pattern of epithelial-mesenchymal transition (EMT) marker expression. The present results demonstrated the significance of TADA3 in regulating the growth and metastasis of NSCLC and may provide a theoretical basis for early diagnosis and targeted therapy of NSCLC.

Key words: transcriptional adaptor 3; non-small cell lung cancer; epithelial-mesenchymal transition; tumorigenesis; cell cycle

Lung cancer is the leading cause of cancer-related deaths worldwide [1], with ~1.4 million deaths annually. Lung cancer can be classified into small cell and non-small cell lung cancer (NSCLC) based on histological features [2, 3]. In total, ~85% of cases are NSCLC, making it one of the most common malignant diseases. More than one-half of patients with NSCLC have distant metastasis at diagnosis, which leads to the majority of human cancer-associated mortalities [4–6], and the 5-year overall survival rate is <15% [7]. Therefore, there is an urgent need to understand the underlying molecular mechanisms that control the proliferative and metastatic phenotypes of NSCLC cells.

Alteration/deficiency in activation (ADA), the human homolog of the yeast transcriptional co-activator NGG1, is a multifunctional protein that participates in a myriad of biological processes, including embryonic development, cellular proliferation, chromatin remodeling, cellular senescence, and DNA damage response. The discovery and designation of yeast ADA3 as a transcriptional co-activator were originally reported in 1992 [8]. ADA3 contains two functionally non-overlapping domains that facilitate its function as a component of histone acetyltransferases (HATs) and transcriptional regulators. The amino-terminal region is required to bind with protein complexes at the upstream activation sequences, and the carboxyl-terminal region is required for recruiting ADA2 and histone acetyltransferase GCN5 (GCN5) complexes in HATs [9–11]. The ternary complex of ADA2, ADA3, and GCN5 forms a catalytic core in HAT complexes, and ADA3 is a pivotal member of HAT complexes in mammals, including PCAF, GCN5, and p300/CBP, similar to NGG1 [12–14]. Epithelial-mesenchymal transition (EMT) is a process by which epithelial cells acquire a mesenchymal phenotype with increased invasive properties [15]. During EMT, genes encoding epithelial cell junction proteins, such as E-cadherin (E-Cad), are downregulated, whereas genes encoding proteins that promote mesenchymal adhesion, such as Vimentin (VIM), N-cadherin (N-Cad), Snail, and Slug (SNAIL+SLUG) are upregulated [16, 17]. A

number of previous studies found that EMT plays a critical role in promoting metastasis of epithelial carcinomas by conferring the potential to invade adjacent tissues and migrate to distant organs [18–22].

In our previous study, a tissue microarray immunohistochemical assay was performed and NSCLC samples showed predominantly cytoplasmic and nuclear locations [23]. Additionally, it was identified that TADA3 is an independent risk factor for the prognosis of patients. In the present study, TADA3 expression in clinical NSCLC specimens and cell lines was examined, and its biological functions in loss-of-function experiments were investigated to explore its involvement in the process of epithelial interstitial transformation. The present study may provide a new potential target for NSCLC and a theoretical basis for subsequent studies.

Patients and methods

Human tissue specimens. Eight pairs of matched tumorous, adjacent normal fresh tissues were collected from NSCLC patients in the Affiliated Hospital of Nantong University, frozen in liquid nitrogen at the time of surgery, and stored at -80 °C. The tissue microarray was derived from the Biobank of the Affiliated Hospital of Nantong University. The study protocol was approved by the Human Research Ethics Committee of the Affiliated Hospital of Nantong University (Ethics approval number: 2018-K020), Jiangsu Province, China. Written informed consent was provided by all participants.

Cell lines and cell culture. The human NSCLC cell lines A549, NCI-H1299, NCI-H1650, and NCI-H1975 were obtained from ScienCell (Carlsbad, CA, USA). Cells were maintained in RPMI-1640 medium (Gibco, USA) supplemented with 10% fetal bovine serum (FBS), 2 mM L-glutamine, and 100 U/ml penicillin/streptomycin, and were cultured in a humidified 5% CO_2 atmosphere at 37 °C. The cells used in the experiment were third to seventh generations after thawing. Cell identification and mycoplasma testing reports are provided by the institution where the cell lines were purchased. All experiments were performed with exponentially growing cells.

Multiplex fluorescent immunohistochemistry (mIHC) staining and imaging. The tissue microarray blocks were baked at 65 °C, dewaxed with xylene, and hydrated with ethanol. After antigen retrieval with a microwave and blocking, the slides were incubated with the primary and secondary antibodies. The signal was amplified by fluorescent-labeled TSA (tyrosine signal amplification, Akoya Biosciences, USA), and the primary and secondary antibodies were removed by a microwave. The above steps from blocking to removal were repeated and the slides were then dyed with Fluoroshield Mounting Medium containing DAPI (F6057, Sigma, USA). Imaging was performed using the Vectra multispectral imaging system (version 3.0, PerkinElmer, USA).

The primary antibody used in this study was anti-ADA3L (ab181984, Abcam, Cambridge, UK), and the secondary antibody was Opal™ poly HRP Ms+Rb (ARH1001EA, Perkin Elmer, China). Fluoroshield with DAPI (F6057, Sigma) was used to stain nuclei and seal the slices.

Cell growth and viability assay. Cells were seeded in 96-well plates at 3×10^3 cells/well and analyzed for viability and growth using a Cell Counting Kit-8 (CCK-8, Beyotime Institute of Biotechnology, Shanghai, China) according to the manufacturer's protocol. At each time point (24–96 h), 10 µl of CCK-8 solution was added to each well and the plates were incubated for 1.5 h at 37 °C. The absorbance at 450 nm was then measured in a microplate spectrophotometer (Synergy HT, BioTek, USA).

Cell migration and invasion assays. These assays were performed using Transwell chambers (353097, Falcon, USA). For the invasion assay, the inserts were pre-coated on the upper surface with Matrigel (BD Biosciences, San Jose, CA, USA) according to the manufacturer's instructions. After 4 h, 5×10^4 cells were added to the upper chamber in serum-free RPMI-1640 medium and the lower chamber was filled with 0.6 ml RPMI-1640 containing 10% FBS as a chemoattractant. After 24 h incubation at 37 °C, the non-invading cells on the upper surface of the membrane were gently removed with a cotton swab, and the invading cells on the lower surface were fixed with 4% paraformaldehyde and stained with 0.3% crystal violet. To quantify invasion, five visual fields (magnification ×200) per insert were randomly selected under a light microscope (Olympus, Japan) and the cells were counted. The experiments were repeated three times. To measure migration, the assay was performed in a similar manner, except the Matrigel coating step was omitted.

Wound-healing assay. Cell migration was also measured using a wound-healing assay. Parental, shControl, or shTADA3 A549 and H1299 cells were seeded in 6-well plates and cultured to 95% confluence. The cell monolayer was then gently scratched with a sterile pipette tip and detached cells were removed by washing once with PBS. Five random fields of cells were photographed and the plates were incubated for 36 h and photographed again. The wound width was measured and the migration rate (MR) was calculated as MR=(D0–D1)/D0, where D0 and D1 represent the wound width at 0 h and 36 h, respectively. The ability of cell migration was detected by the percentage of reduction in wound gap.

Western blot analysis. Cells and tumor tissues were resuspended in lysis buffer (P0013B, Beyotime Institute of Biotechnology) containing 1% protease inhibitor (ST506, Beyotime Institute of Biotechnology). Protein concentrations in the homogenized lysates were measured using the BCA method (BL521A, Biosharp, China). Equal amounts of protein/sample were resolved by SDS-PAGE and then transferred to PVDF membranes (IPVH00010, Millipore Corporation, USA). The membranes were blocked in 5% fat-free milk and incubated overnight at 4 °C with the following primary antibodies: anti-ADA3L (dilution 1:5000, ab181984, Abcam, Cambridge,

UK), anti-E-cadherin (1:10000, ab40772, Abcam), anti-N-cadherin (1:5000, ab76011, Abcam), anti-Vimentin (1:2000, ab92547, Abcam), anti-Snail+Slug (1:2000, ab85936, Abcam), and anti-glyceraldehyde 3-phosphate dehydrogenase (GAPDH; 1:2000, AB0037, Abways). After washing, the membranes were incubated with horseradish peroxidase-conjugated goat anti-rabbit IgG (1:2000, ab205718, Abcam) for 2 h at room temperature. The membranes were then washed again and protein signals were visualized using an ECL system (Bio-Rad, Hercules, CA, USA).

TADA3 silencing and generation of stable cell lines. Four short hairpin RNA sequences targeting human TADA3 used for loss-of-function studies and the sequences had no significant sequence homology with any known gene were designed and obtained from Bioinshine (Shanghai, China). shRNA-1: sense 5'-GGTGACAGACGATTCCTGA-3'; shRNA-2: sense 5'-CCCAAGAAGCAGAAACTGGAA-3'; shRNA-3: sense 5'-CAGCCCAAGATCCAGGAATAT-3'; and shRNA-4: sense 5'-GCTGTGGCTGACAAGAAGAAA-3'. A negative control duplex (shControl, sense: 5'-TTCTCCGAACGTGTCACGT-3') was also synthesized. The sequences were ligated into the PGPH1/GFP/puro vector and transfected into cells. Cells expressing shRNA were identified by monitoring GFP expression. For the selection of stable cell lines, the transfected cells were grown in a medium containing puromycin (Beyotime Institute of Biotechnology) for 30 days, and isolated clones were selected.

RNA extraction and reverse transcription-quantitative PCR (RT-qPCR). Total RNA was extracted from cells with TRIzol reagent (Invitrogen, Carlsbad, CA, USA) and reverse transcribed using a RevertAid First Strand cDNA Synthesis Kit (Thermo Scientific, Vilnius, Lithuania) according to the suppliers' instructions. The following primers for RT-PCR were purchased from Sangon (Shanghai, China): TADA3 forward: 5'-AGATGGATGCCCCTTTGGTG-3', TADA3 reverse: 5'-AGGGCTTGTTCTGATTGCGA-3'; GAPDH forward: 5'-GGTAGACAAGTTTCCCTT-3', GAPDH reverse: 5'-ATATGTTCTGGATGATTCT-3'. qPCR was performed using an ABI 7500 FAST Real-Time PCR System (Applied Biosystems, Carlsbad, CA, USA) and a SYBR Green Master Mix (Vazyme, Nanjing, China). The mRNA levels were quantified using the $2^{-\Delta\Delta Ct}$ method after normalization to GAPDH mRNA.

Cell cycle analysis by flow cytometry. Cell cycle distribution was assessed by staining cells with the PI/RNase Staining Buffer (BD Biosciences). NSCLC cell lines were transfected with shControl or shTADA3 in 6-well plates and harvested 48 h later. Cells were fixed with 70% ethanol and frozen at –20 °C until analysis. For analysis, the cells were collected, washed once with phosphate-buffered saline (PBS), and incubated in 0.5 ml of staining buffer containing PI and RNase for 15 min at room temperature in the dark. Cells were analyzed using a BD FACSCalibur™ flow cytometer (BD Biosciences) and the proportions of cells in each phase of the cell cycle were counted and compared with ModFit LT software.

Tumorigenicity in nude mice. Parental, shControl, or shTADA3 A549 cells were injected subcutaneously (5×10^6 in 100 µl PBS) into male BALB/c athymic nude mice (4 weeks of age) purchased from the Shanghai Experimental Animal Center, Chinese Academy of Sciences (Shanghai, China). After visible tumors had formed, tumor sizes were measured with vernier calipers every 3 days. The tumor volume was calculated as: $V = \text{width}^2 \times \text{length} \times 0.5$. At the end of the experiment, tumors were excised. One portion of each tumor was fixed in 10% formalin and subjected to routine histological examination by a professional who was blinded to the tumor status; the remaining tumor portions were frozen at –80 °C for western blot analysis. All mouse experiments carried out in this project were following the NIH Guidelines with the ethical approval of the Administration Committee of Experimental Animals, Jiangsu Province, China (SYXK2017-0046).

Statistical analysis. Data are shown as the mean ± SD from at least three experiments. Group differences were evaluated with paired Student's t-test or ANOVA analysis. All analyses were completed with the GraphPad Prism software (version 6.01; GraphPad, La Jolla, CA, USA). The value of $p<0.05$ was considered statistically significant.

Results

TADA3 expression in NSCLC tissues and cell lines. To assess TADA3 protein expression in clinical specimens, western blot analysis of eight pairs of matched NSCLC and adjacent non-cancerous tissues was performed. As shown in Figures 1A and 1B, TADA3 was detected at significantly higher levels in all NSCLC tissues compared with normal lung tissues, which is consistent with the result of our previous research [23]. According to mIHC (Figure 1C), TADA3 protein was mainly expressed in the cytoplasm of lung cancer cells, and further proved its higher expression in cancer tissue.

For the *in vitro* analysis, four commonly employed NSCLC cell lines (A549, H1299, H1650, and H1975) were used. While the TADA3 protein and mRNA expression levels were detectable in all four lines, the highest levels were observed in H1299 and A549 cells (Figures 1D–1F). Therefore, these two lines were selected for more detailed loss-of-function experiments.

To select a suitable TADA3-specific shRNA, H1299 cells were transfected with one of four different TADA3-specific shRNAs or a negative control shRNA and TADA3 expression was quantified by western blot analysis (Figures 1G, 1H) or RT-qPCR analysis (Figure 1I). These experiments identified shRNA-1 as being the most effective suppressor of TADA3 mRNA and protein expression.

Silencing of TADA3 delays the cell cycle and inhibits the proliferation of NSCLC cells. The involvement of TADA3 in NSCLC cell proliferation was examined *in vitro* by a CCK-8 assay. Compared with the expression of the control shRNA,

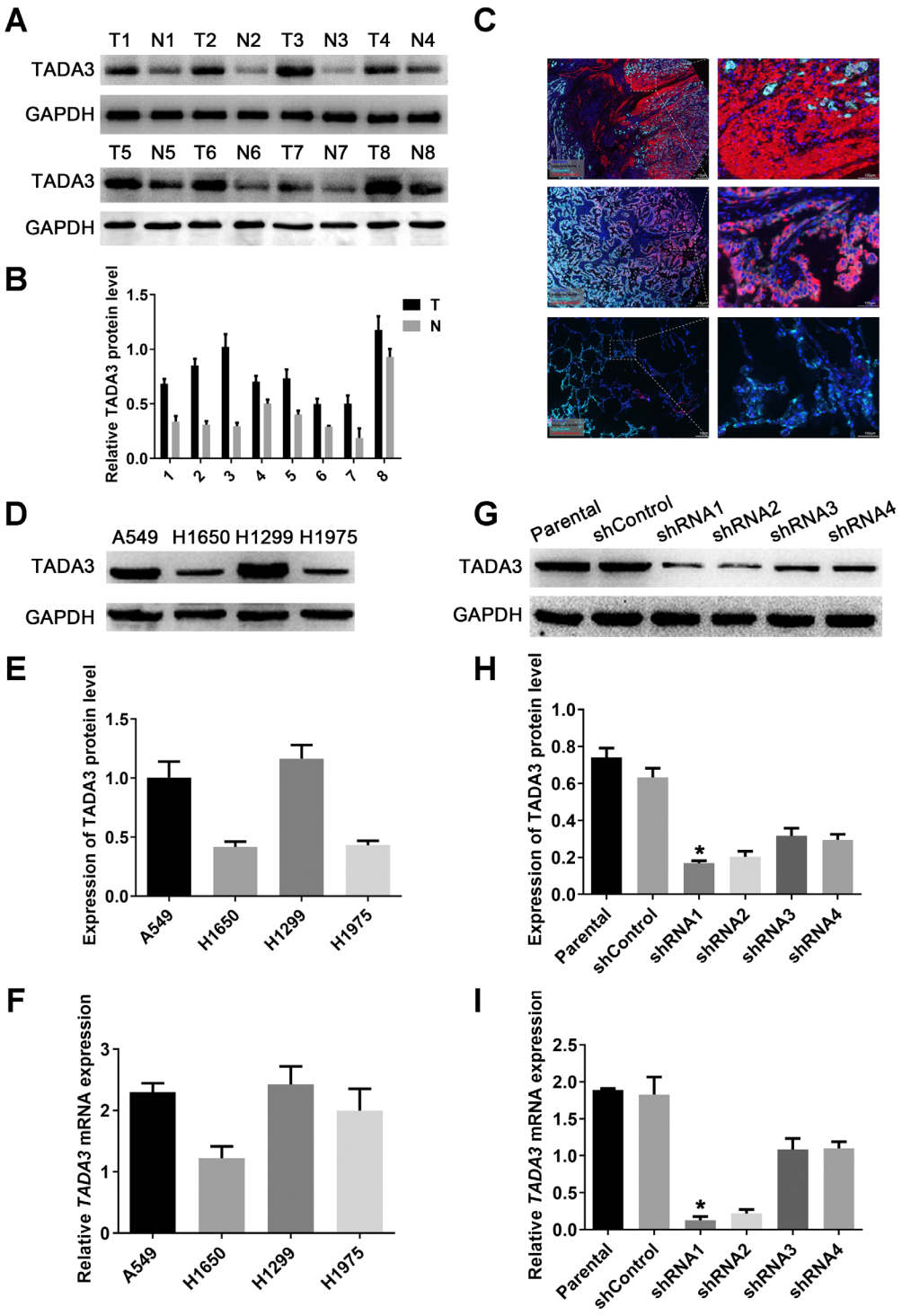

Figure 1. Expression of TADA3 in human NSCLC tissues and cell lines. A) Western blot analysis and B) quantification of TADA3 protein expression in eight pairs of matched normal human lung tissues (lanes labeled with 'N') and NSCLC tissues (lanes labeled with 'T'). GAPDH was used as a loading control. *p<0.05 vs. the normal tissues. C) Representative images of mIHC which were stained by red (TADA3), blue (DAPI), green (CK). The upper two are adenocarcinoma tissues, the middle two are squamous cell carcinoma tissues, and the lower two are normal lung tissues. D) Western blot analysis and E) quantification of TADA3 protein expression in A549, H1299, H1650, and H1975 human NSCLC cell lines. G) Western blot analysis and H) relative quantification of TADA3 expression in H1299 cells expressing control shRNA or one of four TADA3-specific shRNAs (shRNA1-4). F, I) Reverse transcription-quantitative PCR analysis of TADA3 mRNA levels in the NSCLC cell lines treated as described in (D) and (G), respectively. Data are presented as the mean ± SD from three independent experiments. *p<0.001 vs. the negative control. NSCLC, non-small cell lung cancer; TADA3, alteration/deficiency in activation 3; shRNA, short hairpin RNA

shTADA3 transfection markedly reduced the proliferation of all four NSCLC cell lines between 24 and 96 h (Figure 2A). To confirm these results, the percentage of cells in each phase of the cell cycle was analyzed by the flow cytometry analysis of PI-stained cells. The results showed that TADA3 knockdown caused an accumulation of cells in G0/G1 and a reduction of cells in the S phase, indicative of a delay in the G0/G1 to S transition in both H1299 (Figures 2B, 2D) and A549 (Figures 2C, 2E) cells.

Silencing of TADA3 inhibits cell migration and invasion. As the development of migratory and invasive phenotypes is a pivotal step in the process of tumor metastasis, the effect of TADA3 knockdown on these properties was assessed by wound-healing and Transwell assays. The results indicated that TADA3 knockdown significantly reduced A549 (Figures 3A, 3B) and H1299 (Figures 3C, 3D) cell migration. As shown in Figures 3E and 3F, Transwell migration assays further demonstrated the effect of TADA3 on the migration of H1299 and A549 cells. Similarly, Matrigel invasion assays revealed a significant decrease in the invasive capacity of H1299 (Figure 3G) and A549 (Figure 3H) cells expressing shTADA3 compared with shControl or parental cells.

TADA3 regulates EMT markers *in vitro*. EMT is a crucial event in tumorigenesis because epithelial cells lose traits such as cell-cell adhesion and polarity, and acquire a more motile mesenchymal phenotype. To determine whether suppression of TADA3 in NSCLC cells modulates the expression of typical EMT markers, their levels in parental, shControl-expressing, and shTADA3-expressing A549 and H1299 cells were compared. Western blot analysis indicated that TADA3 knockdown upregulated the expression of E-cadherin and downregulated the expression of Vimentin, N-cadherin, Snail, and Slug (Figure 4A). Quantification of the protein levels further demonstrated that TADA3 silencing significantly altered the expression of the EMT markers (Figures 4B, 4C), suggesting that this protein plays an important role in promoting metastasis-associated behavior.

Silencing of TADA3 inhibits tumorigenicity of NSCLC cells *in vivo*. To verify the significance of the *in vitro* observations, the effects of TADA3 knockdown on NSCLC tumor growth were examined *in vivo*. Parental, shControl-expressing, and shTADA3-expressing A549 cell lines were injected subcutaneously into BALB/c nude mice to establish xenografts. The growth rate of xenografts formed from shTADA3-silenced cells grew at significantly slower rates than the tumors formed by control cells *in vivo*. Repression of TADA3 resulted in the development of markedly reduced tumor volumes than the normal and control groups, as presented in Figure 5A. The growth curves also showed that the tumor volume in the TADA3-silenced groups increased more smoothly compared with the normal and control mice (Figure 5B). The results demonstrated that TADA3 showed a definite function in the onset and development of NSCLC *in vivo*.

Additionally, the expressions of metastasis-associated proteins in NSCLC tumors excised from mice were assessed. Consistent with the observations in the NSCLC cell lines grown *in vitro*, it was observed that the tumors derived from TADA3 knockdown cells expressed significantly higher levels of E-cadherin and significantly lower levels of N-cadherin, Vimentin, Snail, and Slug, compared with the parental or shControl cell lines (Figures 5C, 5D).

Discussion

Identification of molecular biomarkers for cancer, including NSCLC, is currently the subject of intense research. Such biomarkers are crucial for predicting the potential risk of disease recurrence and the prognosis of patients with cancer [24, 25]. The aim of the present study was to identify potential molecular markers for the early diagnosis and treatment of NSCLC. It was previously demonstrated that a high expression of TADA3 protein was correlated with a poor prognosis in patients with NSCLC [23]. In the present study, the expression of TADA3 in NSCLC tissue samples was examined and it was identified that this protein was significantly increased in cancer tissue compared with adjacent normal lung tissue.

Mirza et al. [26] proposed that predominant nuclear localization of ADA3 in breast cancer tissues correlates with the ER expression status and together can serve as helpful markers of prognosis, whereas predominant cytoplasmic localization of ADA3 correlates with ErbB2+/EGFR+ expression and together may be used as a better predictor of poor prognosis than the individual proteins. ADA3 plays a key role in recruiting ER and three HATs (p300, PCAF, and Gcn5) to the ER-responsive promoter pS2, and this may transactivate the downstream target genes [14]. It is noteworthy that the knockdown of ADA3 induces ER-mediated proliferation and reversion of the malignant phenotype of MCF-7 cells. ADA3 has been shown to interact with other various proteins associated with tumorigenesis, including HPV16 E6 protein [27, 28] and p53 [29, 30]. Additionally, a number of previous studies have identified alterations in ADA3 as contributing factors in diverse cancer types [31]. However, to the best of the authors' knowledge, relatively few studies have investigated the potential contribution of TADA3 to NSCLC.

Human ADA3 is a multifunctional protein, which is evolutionarily conserved and has diverse cellular functions, including proliferation [32], senescence [33], apoptosis [34], chromatin remodeling [10, 35], and genomic stability [36]. The present study demonstrated that TADA3 is crucial to the proliferation and invasion of NSCLC cells, which are key phenotypes in promoting the growth and metastasis of this tumor.

During mitosis, ADA3 is associated with centromere protein B (CENP-B); the knockdown of ADA3 reduces CENP-B binding to centromeres, suggesting a role for ADA3 in regulating genomic stability and cell proliferation [32,

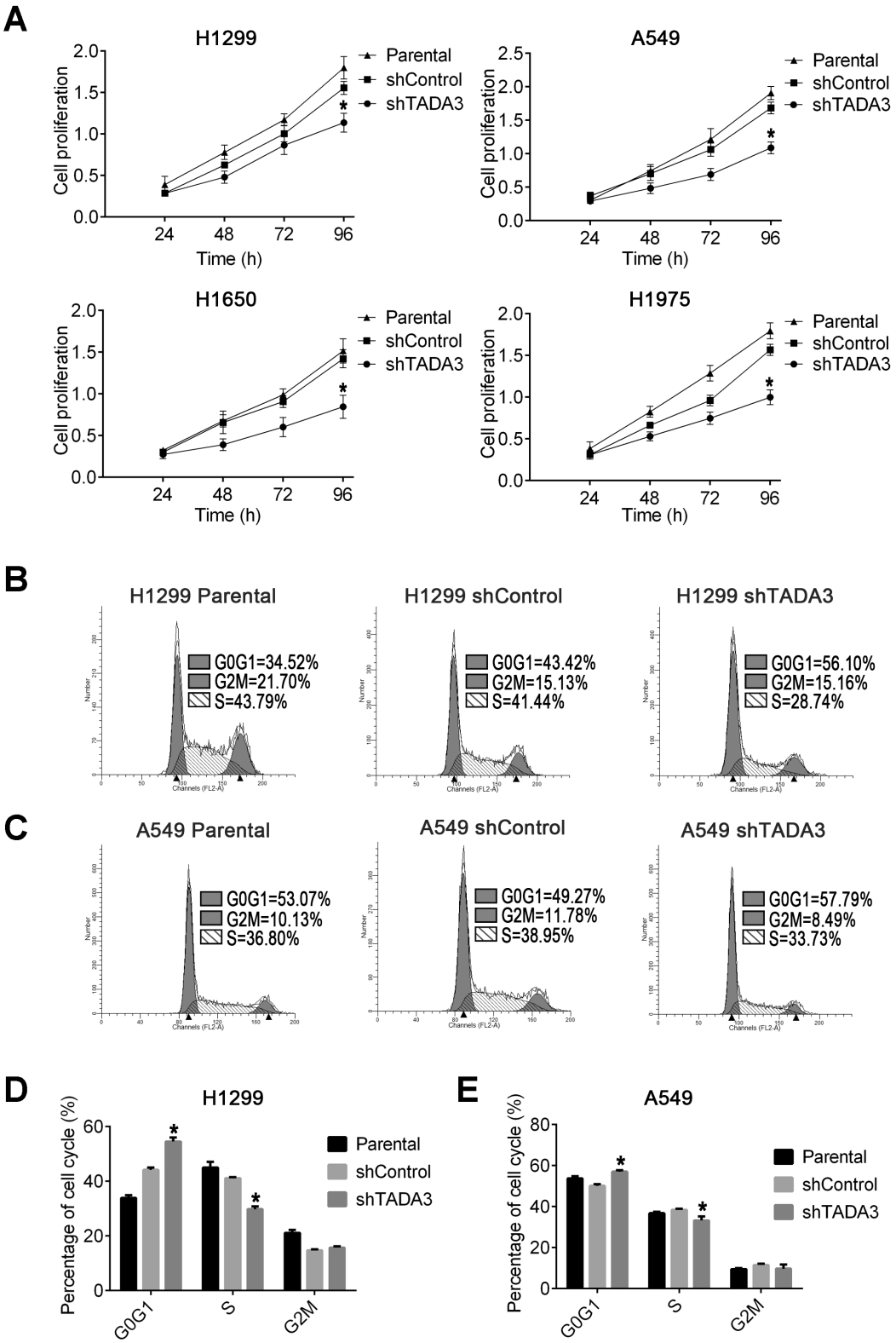

Figure 2. TADA3-mediated regulation of non-small cell lung cancer cell proliferation *in vitro*. A) Cell Counting Kit-8 proliferation assay of parental, shControl-expressing, and shTADA3-expressing A549, H1299, H1650, and H1975 cells over 96 h. B, C) Flow cytometric analysis and D, E) quantification of the cell cycle distribution of parental, shControl-expressing, and shTADA3-expressing H1299 and A549 cells. Data are presented as the mean ± SD from three independent experiments. *p<0.05 vs. the negative control. TADA3, alteration/deficiency in activation 3; sh, short hairpin

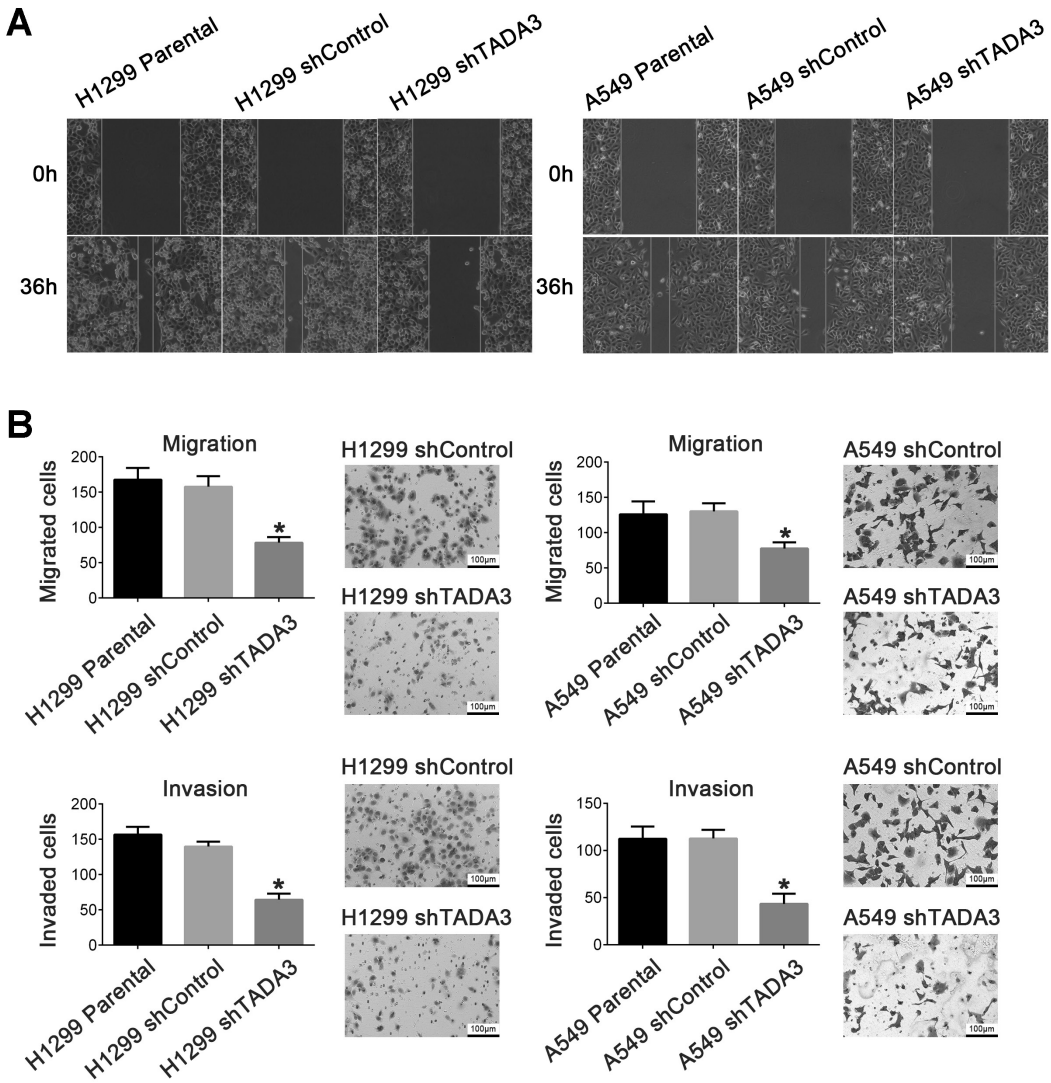

Figure 3. TADA3-mediated regulation of NSCLC cell migration and invasion, and expression of epithelial-mesenchymal transition markers *in vitro*. Representative images of the wound-healing assay of parental, shControl-expressing, and shTADA3-expressing (A) H1299 and (C) A549 cells. Magnification, ×100. B, D) Wound width was measured and the MR was calculated as MR = (D0–D1)/D0, where D0 and D1 represent the wound width at 0 and 36 h, respectively. Plotting histograms according to the percentage of reduction in wound gap. Representative images of transwell migration assays of parental, shControl-expressing, and shTADA3-expressing E) H1299 and F) A549 cells. Magnification, ×200. Quantification of the Matrigel invasion assays of parental, shControl-expressing, and shTADA3-expressing G) H1299 and H) A549 cells. Magnification, ×200. Data are presented as the mean ± SD from three independent experiments. *p<0.01 vs. the negative control. TADA3, alteration/deficiency in activation 3; NSCLC, non-small cell lung cancer; MR, migration rate; sh, short hairpin

37]. Notably, a combined delayed progression of the cells from the G1 to S phase and from the G2/M to G1 phase is displayed in mouse embryonic fibroblasts from ADA3FL/FL mice, supporting the involvement of ADA3 in cell cycle progression. A possible mechanism for this is the accumulation of p27, which is controlled by Myc-dependent regulation of S-phase kinase-associated protein 2 expression [38]. Furthermore, the loss of ADA2a and ADA3 negatively influences β-catenin-mediated proliferation [39]. Consistently, it was demonstrated that TADA3 may have a potential and significant role in promoting cell cycle progression in NSCLC cells in the present study.

To identify potential therapeutic targets for NSCLC, further understanding of the molecular mechanisms underlying invasion and metastasis is required. In the present study, the potential involvement of ADA3 in regulating EMT was investigated. E-cadherin is expressed in epithelial tissues and its absence may serve a key role in EMT [40, 41]. The expression of mesenchymal markers, such as N-cadherin, Snail, and Slug, was previously shown to correlate with poor

survival in patients with NSCLC [42–44]. In the present study, it was observed that silencing of TADA3 in NSCLC cells significantly altered the expression of EMT-related proteins, consistent with its effects on cell migration and invasion assays.

Overall, the expression level of TADA3 in NSCLC tissues is markedly higher compared with adjacent normal lung tissues. Loss-of-function analyses demonstrated that TADA3 promoted the proliferation, migration, and invasion of NSCLC cells. Notably, TADA3 facilitated metastasis of NSCLC cells by upregulating E-cadherin and downregulating N-cadherin, Snail, and Slug. Collectively, these results provide insight into the potential carcinogenic role of TADA3 in NSCLC.

There are still some limitations in our research, the number of tissue samples is small. However, we have confirmed that TADA3 is highly expressed in NSCLC tissues through a large sample of TMA-IHC analysis. We were dedicated to finding the basic functions of TADA3 in NSCLC in this study and in-depth research is worth further exploring.

As a transcriptional co-activator, ADA3 functions to increase RNA polymerase II-mediated gene transcription by recruiting transcription factors or basal transcription machinery to target gene promoters [45]. Co-activator proteins, generally only found in eukaryotes, are more complex than activators and require a more intricate and complicated mechanism for gene regulation [46–49]. Some co-activators, such as GCN5, p300, and CBP, have innate HAT activity and can directly participate in chromatin remodeling. Since ADA3 lacks a HAT domain, it will be interesting to determine which proteins it interacts with as a functional co-activator in NSCLC [47, 50].

Additional transcriptional activators have been found to be targets of the ADA3 co-activator function. The human papillomavirus (HPV) E6 protein targets ADA3 to inhibit its co-activator function for estrogen receptor (ER)-mediated

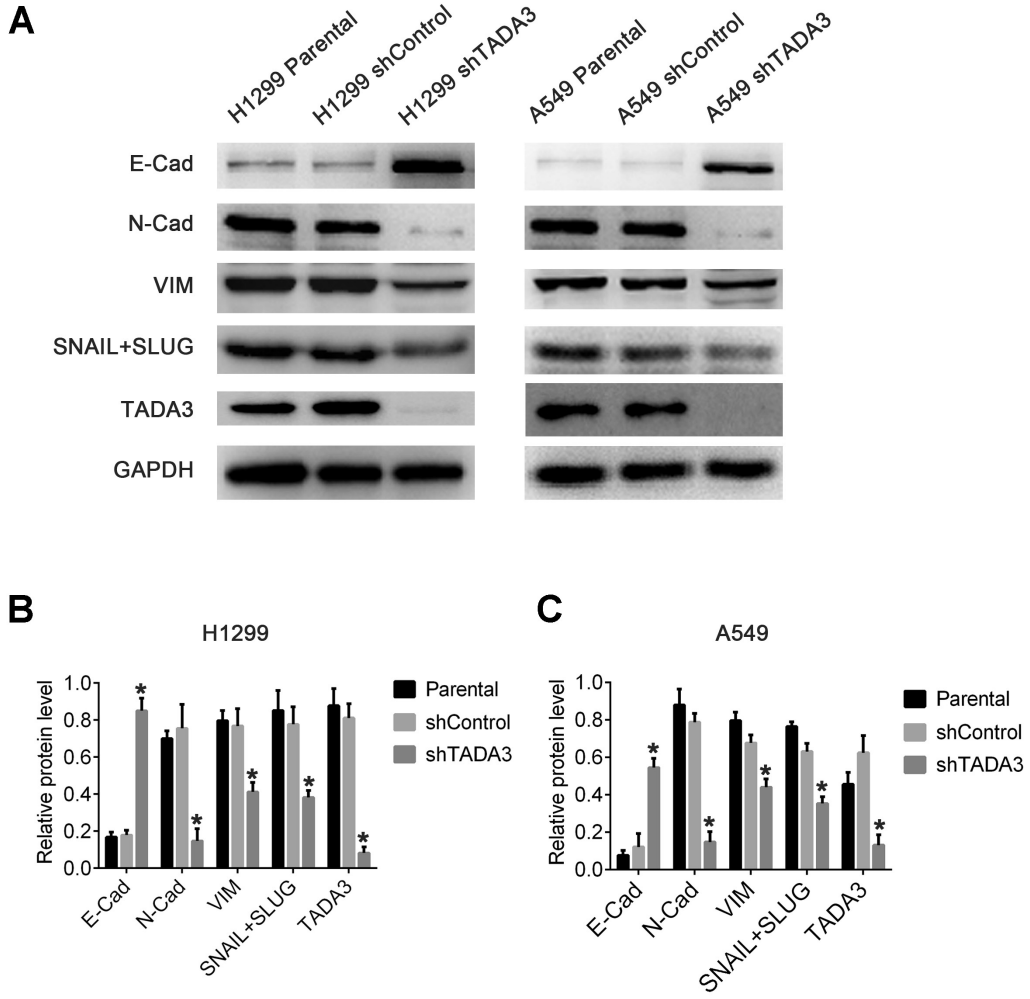

Figure 4. TADA3-mediated regulation of expression of the EMT markers *in vitro*. A) Western blot analysis and B, C) quantification of the expression of the indicated EMT markers (E-Cad, N-Cad, VIM, and SNAIL+SLUG) in parental, shControl-expressing, and shTADA3-expressing H1299 and A549 cells. Data are presented as the mean ± SD from three independent experiments. *p<0.01 vs. the negative control. TADA3, alteration/deficiency in activation 3; EMT, epithelial-mesenchymal transition; sh, short hairpin; E-Cad, E-cadherin; N-Cad, N-cadherin; VIM, vimentin

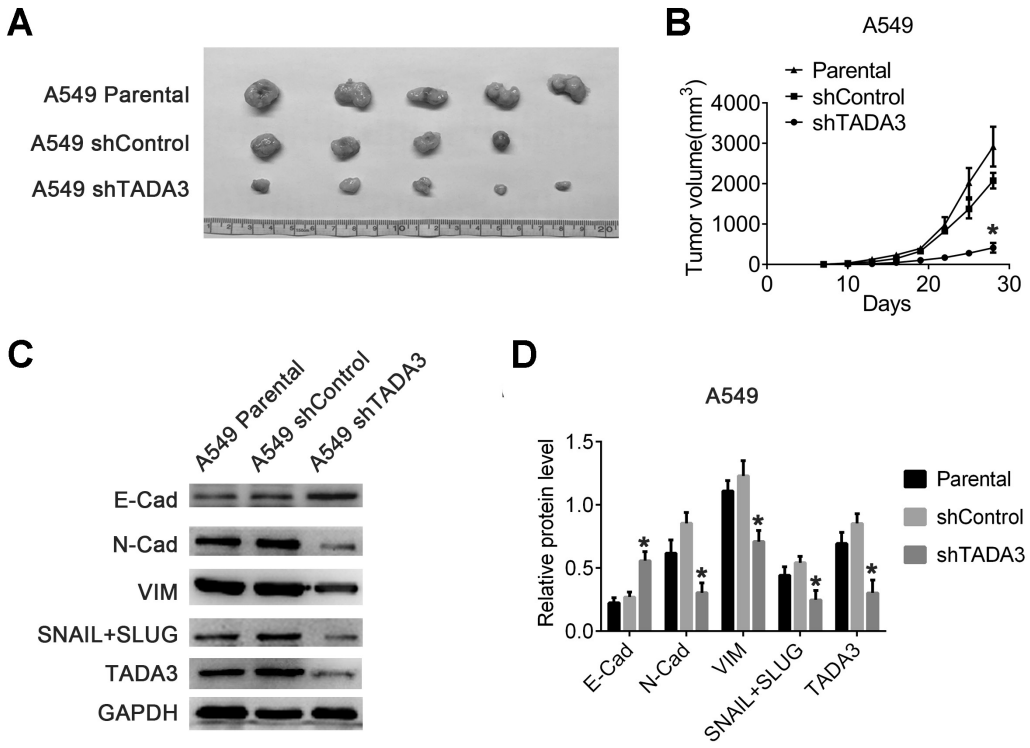

Figure 5. TADA3-mediated regulation of non-small cell lung cancer tumorigenicity and expression of the EMT markers in a tumor xenograft model. A) Representative images and B) growth curves of tumors from nude mice injected with parental, shControl-expressing, and shTADA3-expressing A549 cells. C) Western blot analysis and D) quantification of the indicated EMT markers (E-Cad, N-Cad, VIM, and SNAIL+SLUG) in parental, shControl-expressing, and shTADA3-expressing A549 cells. Data are presented as the mean ± SD from three independent experiments. *p<0.05 vs. the negative control. TADA3, alteration/deficiency in activation 3; EMT, epithelial-mesenchymal transition; sh, short hairpin; E-Cad, E-cadherin; N-Cad, N-Cadherin; VIM, vimentin

transactivation and expression of ER target genes [51]. In breast cancer cells, ADA3 interacts with and transactivates ER-mediated downstream targets, and ADA3 knockdown in the ER+ breast cancer cell line MCF-7 reduced cell proliferation as well as small colonies in Matrigel growth medium, indicating a critical role for ADA3 in recruiting HATs to the promoters of estrogen-responsive target genes and for the estrogen-dependent proliferation of breast cancer cells [14, 52]. Notably, the predominant localization of ADA3 in the cytoplasm was found to be a marker of a poor prognosis in ER+, receptor tyrosine-protein kinase ErbB-2 (ErbB2)+/epidermal growth factor receptor (EGFR)+ breast cancer [26]. Additionally, ADA3 has been shown to interact with ADA2a and β-catenin through its Armadillo repeat sequences 6–10 and C-terminal domain, thereby enhancing the transcriptional activity of the β-catenin response element LEF/TCF [39].

The development of cancer involves multiple genetic and epigenetic steps that transform normal cells into tumor cells. Given the multiple biological functions of TADA3, it is not surprising that it has become of increasing interest to cancer researchers. Further studies are necessary to explore the relationships between TADA3 and other transcriptional regulators involved in tumorigenesis. Further studies may aim to investigate the role of TADA3 in recruiting transcription factors to promote the expression of tumorigenic genes, which may provide further insight into the therapeutic potential of TADA3.

Acknowledgments: We thank the patients and their families for providing consent for the use of tissue samples. The study was supported by grants from the Nantong Municipal Technology Project [MS12022020] and the Project of Nantong Municipal Health Commission [QN2022004].

References

[1] SIEGEL RL, MILLER KD, FUCHS HE, JEMAL A. Cancer statistics, 2022. CA Cancer J Clin 2022; 72: 7–33. https://doi.org/10.3322/caac.21708

[2] CRONIN KA, SCOTT S, FIRTH AU, SUNG H, HENLEY SJ et al. Annual report to the nation on the status of cancer, part 1: National cancer statistics. Cancer 2022; 128: 4251–4284. https://doi.org/10.1002/cncr.34479

[3] ZENG L, YU X, YU T, XIAO J, HUANG Y. Interventions for smoking cessation in people diagnosed with lung cancer. Cochrane Database Syst Rev 2015: CD011751. https://doi.org/10.1002/14651858.CD011751.pub2

[4] CAI C, SHI R, GAO Y, ZENG J, WEI M et al. Reduced expression of sushi domain containing 2 is associated with progression of non-small cell lung cancer. Oncol Lett 2015; 10: 3619–3624. https://doi.org/10.3892/ol.2015.3737

[5] MOUNTAIN CF. The international system for staging lung cancer. Semin Surg Oncol 2000; 18: 106–115. https://doi.org/10.1002/(sici)1098-2388(200003)18:2<106::aid-ssu4>3.0.co;2-p

[6] RICHARD PJ, RENGAN R. Oligometastatic non-small-cell lung cancer: current treatment strategies. Lung Cancer (Auckl) 2016; 7: 129–140. https://doi.org/10.2147/LCTT.S101639

[7] XIAO Z, WANG C, ZHOU R, HU S, YI N et al. Can Aidi injection improve overall survival in patients with non-small cell lung cancer? A systematic review and meta-analysis of 25 randomized controlled trials. Complement Ther Med 2018; 37: 50–60. https://doi.org/10.1016/j.ctim.2018.01.011

[8] BERGER SL, PIñA B, SILVERMAN N, MARCUS GA, AGAPITE J et al. Genetic isolation of ADA2: a potential transcriptional adaptor required for function of certain acidic activation domains. Cell 1992; 70: 251–265. https://doi.org/10.1016/0092-8674(92)90100-q

[9] SYNTICHAKI P, THIREOS G. The Gcn5.Ada complex potentiates the histone acetyltransferase activity of Gcn5. J Biol Chem 1998; 273: 24414–24419. https://doi.org/10.1074/jbc.273.38.24414

[10] BALASUBRAMANIAN R, PRAY-GRANT MG, SELLECK W, GRANT PA, TAN S. Role of the Ada2 and Ada3 transcriptional coactivators in histone acetylation. J Biol Chem 2002; 277: 7989–7995. https://doi.org/10.1074/jbc.M110849200

[11] RISS A, SCHEER E, JOINT M, TROWITZSCH S, BERGER I et al. Subunits of ADA-two-A-containing (ATAC) or Spt-Ada-Gcn5-acetyltrasferase (SAGA) Coactivator Complexes Enhance the Acetyltransferase Activity of GCN5. J Biol Chem 2015; 290: 28997–29009. https://doi.org/10.1074/jbc.M115.668533

[12] OGRYZKO VV, KOTANI T, ZHANG X, SCHILTZ RL, HOWARD T et al. Histone-like TAFs within the PCAF histone acetylase complex. Cell 1998; 94: 35–44. https://doi.org/10.1016/s0092-8674(00)81219-2

[13] MARTINEZ E, PALHAN VB, TJERNBERG A, LYMAR ES, GAMPER AM et al. Human STAGA complex is a chromatin-acetylating transcription coactivator that interacts with pre-mRNA splicing and DNA damage-binding factors in vivo. Mol Cell Biol 2001; 21: 6782–6795. https://doi.org/10.1128/MCB.21.20.6782-6795.2001

[14] GERMANIUK-KUROWSKA A, NAG A, ZHAO X, DIMRI M, BAND H et al. Ada3 requirement for HAT recruitment to estrogen receptors and estrogen-dependent breast cancer cell proliferation. Cancer Res 2007; 67: 11789–11797. https://doi.org/10.1158/0008-5472.CAN-07-2721

[15] LAMOUILLE S, XU J, DERYNCK R. Molecular mechanisms of epithelial-mesenchymal transition. Nat Rev Mol Cell Biol 2014; 15: 178–196. https://doi.org/10.1038/nrm3758

[16] DAI X, XIN Y, XU W, TIAN X, WEI X et al. CBP-mediated Slug acetylation stabilizes Slug and promotes EMT and migration of breast cancer cells. Sci China Life Sci 2021; 64: 563–574. https://doi.org/10.1007/s11427-020-1736-5

[17] KIM BN, AHN DH, KANG N, YEO CD, KIM YK et al. TGF-β induced EMT and stemness characteristics are associated with epigenetic regulation in lung cancer. Sci Rep 2020; 10: 10597. https://doi.org/10.1038/s41598-020-67325-7

[18] TSAI JH, YANG J. Epithelial-mesenchymal plasticity in carcinoma metastasis. Genes Dev 2013; 27: 2192–2206. https://doi.org/10.1101/gad.225334.113

[19] VAN ZIJL F, MALL S, MACHAT G, PIRKER C, ZEILLINGER R et al. A human model of epithelial to mesenchymal transition to monitor drug efficacy in hepatocellular carcinoma progression. Mol Cancer Ther 2011; 10: 850–860. https://doi.org/10.1158/1535-7163.MCT-10-0917

[20] YANG AD, CAMP ER, FAN F, SHEN L, GRAY MJ et al. Vascular endothelial growth factor receptor-1 activation mediates epithelial to mesenchymal transition in human pancreatic carcinoma cells. Cancer Res 2006; 66: 46–51. https://doi.org/10.1158/0008-5472.CAN-05-3086

[21] LEE KW, KIM JH, HAN S, SUNG CO, DO IG et al. Twist1 is an independent prognostic factor of esophageal squamous cell carcinoma and associated with its epithelial-mesenchymal transition. Ann Surg Oncol 2012; 19: 326–335. https://doi.org/10.1245/s10434-011-1867-0

[22] XU X, ZHU Y, LIANG Z, LI S, XU X et al. c-Met and CREB1 are involved in miR-433-mediated inhibition of the epithelial-mesenchymal transition in bladder cancer by regulating Akt/GSK-3β/Snail signaling. Cell Death Dis 2016; 7: e2088. https://doi.org/10.1038/cddis.2015.274

[23] ZHANG S, XU L, TANG Z, WANG H, GU J et al. Overexpression of Alteration/Deficiency in Activation 3 correlates with poor prognosis in non-small cell lung cancer. Pathol Res Pract 2019; 215: 152408. https://doi.org/10.1016/j.prp.2019.03.036

[24] WOODARD GA, JONES KD, JABLONS DM. Lung Cancer Staging and Prognosis. Cancer Treat Res 2016; 170: 47–75. https://doi.org/10.1007/978-3-319-40389-2_3

[25] SUZUKI K, KACHALA SS, KADOTA K, SHEN R, MO Q et al. Prognostic immune markers in non-small cell lung cancer. Clin Cancer Res 2011; 17: 5247–5256. https://doi.org/10.1158/1078-0432.CCR-10-2805

[26] MIRZA S, RAKHA EA, ALSHAREEDA A, MOHIBI S, ZHAO X et al. Cytoplasmic localization of alteration/deficiency in activation 3 (ADA3) predicts poor clinical outcome in breast cancer patients. Breast Cancer Res Treat 2013; 137: 721–731. https://doi.org/10.1007/s10549-012-2363-3

[27] ZENG M, KUMAR A, MENG G, GAO Q, DIMRI G et al. Human papilloma virus 16 E6 oncoprotein inhibits retinoic X receptor-mediated transactivation by targeting human ADA3 coactivator. J Biol Chem 2002; 277: 45611–45618. https://doi.org/10.1074/jbc.M208447200

[28] ECKNER R, LUDLOW JW, LILL NL, OLDREAD E, ARANY Z et al. Association of p300 and CBP with simian virus 40 large T antigen. Mol Cell Biol 1996; 16: 3454–3464. https://doi.org/10.1128/MCB.16.7.3454
[29] NAG A, GERMANIUK-KUROWSKA A, DIMRI M, SASSACK MA, GURUMURTHY CB et al. An essential role of human Ada3 in p53 acetylation. J Biol Chem 2007; 282: 8812–8820. https://doi.org/10.1074/jbc.M610443200
[30] WANG T, KOBAYASHI T, TAKIMOTO R, DENES AE, SNYDER EL et al. hADA3 is required for p53 activity. EMBO J 2001; 20: 6404–6413. https://doi.org/10.1093/emboj/20.22.6404
[31] CHAND V, NANDI D, MANGLA AG, SHARMA P, NAG A. Tale of a multifaceted co-activator, hADA3: from embryogenesis to cancer and beyond. Open Biol 2016; 6. https://doi.org/10.1098/rsob.160153
[32] MOHIBI S, SRIVASTAVA S, WANG-FRANCE J, MIRZA S, ZHAO X et al. Alteration/Deficiency in Activation 3 (ADA3) Protein, a Cell Cycle Regulator, Associates with the Centromere through CENP-B and Regulates Chromosome Segregation. J Biol Chem 2015; 290: 28299–28310. https://doi.org/10.1074/jbc.M115.685511
[33] SEKARIC P, SHAMANIN VA, LUO J, ANDROPHY EJ. hAda3 regulates p14ARF-induced p53 acetylation and senescence. Oncogene 2007; 26: 6261–6268. https://doi.org/10.1038/sj.onc.1210462
[34] BRASACCHIO D, NOORI T, HOUSE C, BRENNAN AJ, SIMPSON KJ et al. A functional genomics screen identifies PCAF and ADA3 as regulators of human granzyme B-mediated apoptosis and Bid cleavage. Cell Death Differ 2014; 21: 748–760. https://doi.org/10.1038/cdd.2013.203
[35] ZENCIR S, SIKE A, DOBSON MJ, AYAYDIN F, BOROS I et al. Identification of transcriptional and phosphatase regulators as interaction partners of human ADA3, a component of histone acetyltransferase complexes. Biochem J 2013; 450: 311–320. https://doi.org/10.1042/BJ20120452
[36] MIRZA S, KATAFIASZ BJ, KUMAR R, WANG J, MOHIBI S et al. Alteration/deficiency in activation-3 (Ada3) plays a critical role in maintaining genomic stability. Cell Cycle 2012; 11: 4266–4274. https://doi.org/10.4161/cc.22613
[37] KIM Y, HOLLAND AJ, LAN W, CLEVELAND DW. Aurora kinases and protein phosphatase 1 mediate chromosome congression through regulation of CENP-E. Cell 2010; 142: 444–455. https://doi.org/10.1016/j.cell.2010.06.039
[38] MOHIBI S, GURUMURTHY CB, NAG A, WANG J, MIRZA S et al. Mammalian alteration/deficiency in activation 3 (Ada3) is essential for embryonic development and cell cycle progression. J Biol Chem 2012; 287: 29442–29456. https://doi.org/10.1074/jbc.M112.378901
[39] YANG M, WATERMAN ML, BRACHMANN RK. hADA2a and hADA3 are required for acetylation, transcriptional activity and proliferative effects of beta-catenin. Cancer Biol Ther 2008; 7: 120–128. https://doi.org/10.4161/cbt.7.1.5197
[40] VAN ROY F, BERX G. The cell-cell adhesion molecule E-cadherin. Cell Mol Life Sci 2008; 65: 3756–3788. https://doi.org/10.1007/s00018-008-8281-1
[41] ACLOQUE H, ADAMS MS, FISHWICK K, BRONNER-FRASER M, NIETO MA. Epithelial-mesenchymal transitions: the importance of changing cell state in development and disease. J Clin Invest 2009; 119: 1438–1449. https://doi.org/10.1172/JCI38019
[42] PEINADO H, OLMEDA D, CANO A. Snail, Zeb and bHLH factors in tumour progression: an alliance against the epithelial phenotype. Nat Rev Cancer 2007; 7: 415–428. https://doi.org/10.1038/nrc2131
[43] BREMNES RM, VEVE R, GABRIELSON E, HIRSCH FR, BARON A et al. High-throughput tissue microarray analysis used to evaluate biology and prognostic significance of the E-cadherin pathway in non-small-cell lung cancer. J Clin Oncol 2002; 20: 2417–2428. https://doi.org/10.1200/JCO.2002.08.159
[44] DAUPHIN M, BARBE C, LEMAIRE S, NAWROCKI-RABY B, LAGONOTTE E et al. Vimentin expression predicts the occurrence of metastases in non small cell lung carcinomas. Lung Cancer 2013; 81: 117–122. https://doi.org/10.1016/j.lungcan.2013.03.011
[45] COUREY, ALBERT J. Mechanisms in Transcriptional Regulation. 2008. Mechanisms in transcriptional regulation /.
[46] PENNACCHIO LA, BICKMORE W, DEAN A, NOBREGA MA, BEJERANO G. Enhancers: five essential questions. Nat Rev Genet 2013; 14: 288–295. https://doi.org/10.1038/nrg3458
[47] BROWN CE, LECHNER T, HOWE L, WORKMAN JL. The many HATs of transcription coactivators. Trends Biochem Sci 2000; 25: 15–19. https://doi.org/10.1016/s0968-0004(99)01516-9
[48] VOSNAKIS N, KOCH M, SCHEER E, KESSLER P, MéLY Y et al. Coactivators and general transcription factors have two distinct dynamic populations dependent on transcription. EMBO J 2017; 36: 2710–2725. https://doi.org/10.15252/embj.201696035
[49] NÄÄR AM, LEMON BD, TJIAN R. Transcriptional coactivator complexes. Annu Rev Biochem 2001; 70: 475–501. https://doi.org/10.1146/annurev.biochem.70.1.475
[50] VOM BAUR E, HARBERS M, UM SJ, BENECKE A, CHAMBON P et al. The yeast Ada complex mediates the ligand-dependent activation function AF-2 of retinoid X and estrogen receptors. Genes Dev 1998; 12: 1278–1289. https://doi.org/10.1101/gad.12.9.1278
[51] MENG G, ZHAO Y, NAG A, ZENG M, DIMRI G et al. Human ADA3 binds to estrogen receptor (ER) and functions as a coactivator for ER-mediated transactivation. J Biol Chem 2004; 279: 54230–54240. https://doi.org/10.1074/jbc.M404482200
[52] GRIFFIN NI, SHARMA G, ZHAO X, MIRZA S, SRIVASTAVA S et al. ADA3 regulates normal and tumor mammary epithelial cell proliferation through c-MYC. Breast Cancer Res 2016; 18: 113. https://doi.org/10.1186/s13058-016-0770-9